Shuttling of electrons and Cooper pairs

2003 J. Phys.: Condens. Matter 15 R441

(http://iopscience.iop.org/0953-8984/15/12/201)

INSTITUTE OF PHYSICS PUBLISHING JOURNAL OF PHYSICS: CONDENSED MATTER

J. Phys.: Condens. Matter **15** (2003) R441–R469 PII: S0953-8984(03)33489-7

TOPICAL REVIEW

Shuttling of electrons and Cooper pairs

R I Shekhter[1], Yu Galperin[2,3], L Y Gorelik[1], A Isacsson[1] and M Jonson[1]

[1] Department of Applied Physics, Chalmers University of Technology and Göteborg University, SE-412 96 Göteborg, Sweden
[2] Department of Physics, University of Oslo, PO Box 1048 Blindern, N-0316 Oslo, Norway
[3] Division of Solid State Physics, Ioffe Institute of the Russian Academy of Sciences, St Petersburg 194021, Russia

E-mail: shekhter@fy.chalmers.se

Received 6 January 2003
Published 17 March 2003
Online at stacks.iop.org/JPhysCM/15/R441

Abstract

Properties of nanocomposite materials are affected by a coupling between mechanical deformations of the materials and electronic charge transport. In one of the simplest systems of this kind, a single electron transistor (SET) with deformable tunnel barriers (nanoelectromechanical SET), mechanically assisted charge transfer becomes possible. This can be viewed as 'shuttling of single electrons' between metallic leads by a movable small-sized cluster. In this article we review some recent theoretical and experimental achievements concerning shuttle transport, in normal as well as superconducting systems.

Contents

Abbreviations

SET	Single-electron transistor
NEM-SET	Nanoelectromechanical SET

Notation

e	Elementary (electron) charge
n	Number of electrons on metallic island
x	Oscillator displacement from equilibrium position
q	Oscillator charge
m	Oscillator mass
k_0	Effective spring constant
$\omega_0 = \sqrt{k_0/m}$	Natural vibration frequency
$f_0 = \omega_0/2\pi$	Natural vibration frequency (Hz)
$T_0 = 1/f$	Period of vibration
λ	Characteristic tunnelling length
$R_{L,R}(x)$	Position-dependent tunnel resistances between island and (left/right) leads
$C_{L,R}(x)$	Position-dependent capacitances between island and (left/right) leads
ω_R^{-1}	Charge relaxation rate
V	Applied dc bias voltage
V_0	Coulomb-blockade threshold voltage
I	Direct current
T	Temperature

1. Introduction

During recent years, nanotechnology has advanced the ability to fabricate systems in which chemical self-assembly defines the functional and structural units of nanoelectronic devices [1]. Since the elastic parameters of many compounds and devices currently utilized can be much 'softer' than those of semiconductors and metals, mechanical degrees of freedom may play an important role in charge transfer. In particular, charge transfer via tunnelling through a device can be dramatically enhanced by mechanical motion of some part of the device.

The role of nanoelectromechanical coupling in these systems follows immediately from the heteroelastic nature of the materials taken in combination with the important role played by Coulomb correlations in controlling electron tunnelling between metallic clusters. Tunnelling of a single electron between nanometre-sized grains is accompanied by an increase in electrostatic energy which can be of the order of 10% of the atomic binding energy of the material. As a result, significant deformations of the soft dielectric material separating the grains appear. These deformations in turn strongly affect the tunnelling rate of the electrons, which is exponentially sensitive to the tunnelling distance. Such a mutual influence of mechanical displacements and charge redistribution by tunnelling indeed results in a dynamical coupling between mechanical and electronic degrees of freedom. In particular, since the typical times characterizing the dynamics of each of them can be of the same order of magnitude for metal–organic nanocomposites, this coupling cannot be neglected.

As a simple example of a device of the type discussed above, we shall consider a metallic grain elastically suspended between a source and a drain electrode as shown in figure 1. If, due to a fluctuation in the position of the grain, it approaches the source (or drain) electrode, then the tunnelling coupling between the grain and this electrode increases significantly. As a result,

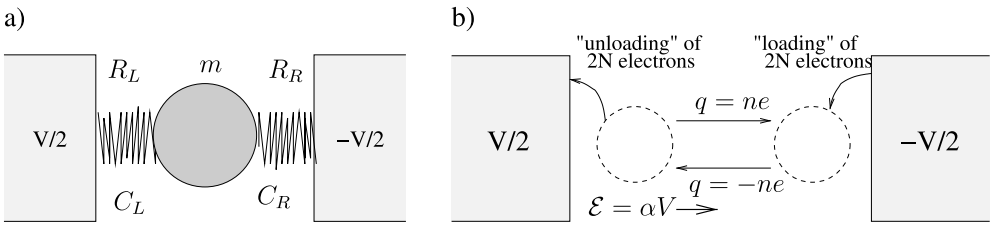

Figure 1. (a) A simple model of a soft Coulomb-blockade system in which a metallic grain (centre) is linked to two electrodes by elastically deformable organic molecular links. (b) A dynamic instability occurs since in the presence of a sufficiently large bias voltage V the grain is accelerated by the corresponding electrostatic force towards first one, then the other electrode. A cyclic change in direction is caused by the repeated 'loading' of electrons near the negatively biased electrode and the subsequent 'unloading' of the same at the positively biased electrode. As a result, the sign of the net grain charge alternates, leading to an oscillatory grain motion and a novel 'electron shuttle' mechanism for charge transport. From [8]. © (1998) by the American Physical Society.

the grain becomes negatively (positively) charged. Then, being now accelerated by elastic and Coulomb electrostatic forces, the grain moves back, approaching the drain (source) electrode, thus transferring the charge. This process, which repeats itself, is usually referred to as shuttling of electrons. In general, the shuttle mechanism can be defined as a charge transfer through a mechanical subsystem facilitated by its oscillatory centre-of-mass motion. The key issue here is that the charge of the grain, $q(t)$, is correlated with its velocity, $\dot{x}(t)$, in such a way that the time-averaged product of charge and velocity is non-zero, $\overline{q(t)\dot{x}(t)} \neq 0$. As a consequence, the average work performed by the electrostatic force does not vanish, even if the average grain velocity does, $\overline{\dot{x}(t)} = 0$. As a result, the system of figure 1 can be unstable with respect to the formation of periodic or quasiperiodic mechanical grain vibrations and hence a periodic or quasiperiodic electrical signal.

Another important feature of nanosystems is the *Coulomb blockade* [2]. A small system which has accepted an electron becomes negatively charged, and under certain conditions another electron cannot, due to Coulomb repulsion, reach the grain. As a result, it has to wait until the first electron has escaped. Until then, further transport is blocked. Thus, under Coulomb-blockade conditions the electrons can be transferred only *one by one*. The smaller the system capacitance, the bigger the charging energy. Consequently, the Coulomb blockade is an intrinsic property of small devices, and its importance increases with the progress in nanoscience and nanotechnology as devices become smaller and smaller. Hence, due to Coulomb blockade, shuttling of *single electrons* or single Cooper pairs can take place.

During the past five years, shuttles of different types have been investigated, both theoretically and experimentally. In particular, it has been found that shuttling can either result from an internal instability similar to the one discussed above, or be achieved by an externally driven motion due to, e.g., some ac electric or mechanical force. Another point is that electron transport through the device can obey the laws of either classical or quantum mechanics. Also the mechanical degrees of freedom can obey either classical or quantum mechanics. Hence, shuttle charge transfer in soft nanostructures involves rich and interesting physics.

At present, many researchers are interested in shuttling in nanoelectromechanical systems, aiming to determine fundamental properties of electromechanical coupling in nanostructures, electron and phonon transport, etc. This knowledge will definitely give renewed impetus to the design of new application devices, such as nanogenerators, nanoswitches, and current standards.

electron transport \ mechanical motion	classical	quantum mechanical
incoherent	**Classical shuttling of particles.** **Sec. 2.1**	**Quantum shuttling of particles** **Sec. 2.3**
coherent	**Classical shuttling of waves** **Sec. 2.2, Sec 4.**	**Quantum shuttling of waves** **Sec. 2.3**

Figure 2. Classification of shuttle transport. Shuttle transport of charge can be classified according to what type of physical description is needed for the mechanical and electronic subsystems.

Shuttle electron transfer can take place not only through a metallic grain, but also through a relatively soft nanocluster. In this connection, it is important to study vibrational modes of electromechanical systems with several degrees of freedom. If the centre-of-mass motion can be clearly split from other modes, then the shuttle electron transfer though the system is similar to that in the case of a rigid grain. Otherwise, it is more appropriate to speak of *vibronically assisted tunnelling* rather than shuttling.

Further, electromechanical coupling with shuttle transport is not only a feature of heteroelastic nanocomposites. It also has, as will be seen below, relevance for other nanoelectromechanical (NEMS) systems intentionally designed to work at the nanometre scale [3–5].

Our aim here is to discuss some of the issues raised above. We will start from the simplest case of a particle with one mechanical degree of freedom located between two electrodes and elastically coupled either to the substrate or to the leads. This situation is relevant to several experiments, e.g., to electron shuttling through an artificial structure [6], and to shuttling through an oscillating C_{60} molecule [7]. Both the classical and quantum electron transport will be considered, in respectively sections 2.1 and 2.2 (see figure 2). It will be shown that in both cases an electromechanical instability occurs which leads to formation of a periodic mechanical motion [8–10]. Section 2.3 aims to review theoretical work regarding the systems where the mechanical degrees of freedom need to be treated quantum mechanically. A review of the available experimental results is given in section 3. Finally, the possibility of coherent shuttling of Cooper pairs between two superconductors through a movable superconducting grain will be considered in section 4.

2. Single-electron transfer by a nanoshuttle

As already mentioned, the shuttle charge transfer involves two processes, the tunnelling coupling between grain and leads and a 'convective' motion performed by the system together with the vibrating grain. To specify the shuttling regime it is natural to compare the characteristic (decay) length λ of the tunnelling coupling with the quantum mechanical zero-point vibration amplitude, $x_0 = \sqrt{\hbar/m\omega_0}$. If $x_0 \ll \lambda$, the mechanical motion can be treated classically. However, the electron transfer through the grain can be either sequential

or coherent. In the first case, the relevant physical picture is fully classical—electrons can be regarded as classical particles, their transport obeying the master equation. We will call this situation the *classical shuttling of particles*. In the case of coherent tunnelling electrons should be treated as wavepackets, keeping track of the properties of their wavefunctions. We will call this situation *classical shuttling of waves* (cf figure 2). The word 'classical' here serves as a reminder that the mechanical motion is classical. In all recent experiments, including shuttling by a C_{60} molecule [7], the condition $x_0 \ll \lambda$ was met. However, a scaling down of the vibrating system can, in principle, lead to violation of this inequality. In that case the mechanical motion also obeys quantum mechanics. We refer to this case as the *quantum shuttling*. In the following sections all three regimes will be considered (see figure 2).

2.1. Classical shuttling of particles

We begin this section by considering the classical shuttling of electrons and specifying the conditions which have to be met for shuttling to fall into this category (section 2.1.1). We then proceed to considering the classical shuttling of electrons by a harmonically bound cluster between two leads in section 2.1.2. After that, since we have seen that low damping is in this case necessary for shuttle transport, a system dominated by viscous forces is considered in 2.1.3. In this case also, classical shuttling of particles take place.

The perspectives of the shuttle for applications depend strongly of several issues. Among them are:

(i) the conditions required for ideal shuttling, which is crucially important for standards of electric current or for sensors;
(ii) gate-induced control of shuttling, important for applications in single-electron transistors;
(iii) the role of mechanical degrees of freedom other than centre-of-mass ones.

These issues will be addressed in sections 2.1.4–2.1.6.

2.1.1. Requirements for incoherent transport. A schematic picture of a single-electron device with a movable metallic cluster is presented in figure 1. Since electronic transport in the device is due to tunnelling between the leads and the central small-size conductor, it is strongly affected by the displacement of the latter. In this case, centre-of-mass mechanical vibrations of the grain will be present (consider the elastic springs, connecting the central electrode to the leads in figure 1).

A number of characteristic times determine the dynamical evolution of the system. Electronic degrees of freedom are represented by frequencies corresponding to such energies as the Fermi energy in each of the conductors and the applied voltage eV. In addition, one has an inverse relaxation time and inverse phase-breaking time for electrons in the conductors, and a tunnelling charge relaxation time $\omega_R^{-1} = RC$. Here R and C respectively are the resistance and capacitance of the tunnel junction. Mechanical degrees of freedom are characterized by a vibration frequency ω_0. The condition that $\hbar\omega_R$ should be much smaller than the Fermi energy is the standard condition for a weak tunnelling coupling and holds very well in usual tunnel structures. Since a finite voltage is supposed to be applied causing a non-equilibrium evolution of the system, the question of electronic relaxation becomes relevant. Two possible scenarios of electronic transfer through the metallic cluster can be identified depending on the ratio between the tunnelling relaxation time ω_R^{-1} and the intra-grain electronic relaxation time τ_0. In the case where τ_0 is much shorter than ω_R^{-1}, the two sequential electron tunnelling events, necessary to transfer an electron from one lead to another through the grain, cannot be considered to be a quantum mechanically coherent process. This is because relaxation and

phase-breaking processes occur in between these events, which are separated by a time of order ω_R^{-1}. Instead, all electronic tunnelling transitions between either lead and the grain can be considered to be incoherent, independent events. Fast relaxation of electrons in all three conductors is assumed to lead to the formation of local (on each of the conductors) equilibrium distributions of electrons. This is the approach which we will use in the present section. In the opposite limit, i.e. when τ_0 is much larger than ω_R^{-1}, quantum coherence plays a dominant role in the electronic charge transfer process and all relaxation takes place in the leads far away from the central part of the device. This case will be considered in section 2.2.

2.1.2. Shuttling of electrical charge by a movable Coulomb dot. The tunnel junctions between the leads and the grain in figure 1 are modelled by tunnelling resistances $R_L(x)$ and $R_R(x)$ which are assumed to be exponential functions of the grain coordinate x. In order to avoid unimportant technical complications we study the symmetric case for which $R_{L,R} = R(0)\mathrm{e}^{\pm x/\lambda}$. When the position of the grain is fixed, the electrical potential of the grain and its charge q_{st} are given by current balance between the grain and the leads [2]. As a consequence, at a given bias voltage V the charge $q_{st}(x)$ is completely controlled by the ratio $R_L(x)/R_R(x)$ and $\mathrm{d}q_{st}(x)/\mathrm{d}x < 0$. In addition the bias voltage generates an electrostatic field $\mathcal{E} = \alpha V$ in the space between the leads and, hence, a charged grain will be subjected to an electrostatic force $F_q = \alpha V q$.

The central point of our considerations is that the grain—because of the 'softness' of the organic molecular links connecting it to the leads—may move and change its position. The grain motion disturbs the current balance and as a result the grain charge will vary over time in tandem with the grain displacement. This variation affects the work $W = \alpha V \int \dot{x} q(t)\,\mathrm{d}t$ performed on the grain during, say, one period of its oscillatory motion.

It is significant that the work is non-zero and positive, i.e., the electrostatic force, on average, accelerates the grain. The nature of this acceleration is best understood by considering a grain oscillating with a frequency which is much smaller than the typical charge fluctuation frequency $\omega_R = 1/RC$ (here C is the capacitance of the metallic cluster which for room temperature Coulomb-blockade systems is of the order of 10^{-18}–10^{-19} F). In this limit the charge deviation $\delta q \equiv (q - q_{st}(x))$ connected with retardation effects is given by the expression $\delta q = -\omega_R^{-1}\dot{x}\,\mathrm{d}q_{st}(x)/\mathrm{d}x$. Hence the extra charge δq depends on the value and direction of the grain velocity and, as a consequence, the grain acts as a shuttle that carries positive extra charge on its way from the positive to the negative electrode and negative extra charge on its return trip. The electrostatic force $\delta F_q = \alpha V\,\delta q$ is thus at all times directed along the line of motion, causing the grain to accelerate. To be more precise, it was shown [8, 9] that for small deviations from equilibrium ($x = 0$, $q = 0$) and provided that $q(t)$ is defined as the linear response to the grain displacement, $q(t) = \int \chi(t - t')x(t')\,\mathrm{d}t'$, the work done on the grain is positive for any relation between the charge fluctuation frequency ω_R and the frequency of the grain vibration.

In any real system a certain amount Q of energy is dissipated due to mechanical damping forces which always exist. In order to get to the self-excitation regime, more energy must be pumped into the system from the electrostatic field than can be dissipated; W must exceed Q. Since the electrostatic force increases with the bias voltage, this condition can be fulfilled if V exceeds some critical value V_c.

If the electrostatic and damping forces are much smaller than the elastic restoring force, self-excitation of vibrations with a frequency equal to the eigenfrequency of the elastic oscillations arises. In this case V_c can be implicitly defined by the relation $\omega_0\gamma = \alpha V_c\,\mathrm{Im}\,\chi(\omega)$, where $\omega_0\gamma$ is the imaginary part of the complex dynamic modulus. In the general case, when the charge response is determined by Coulomb-blockade phenomena, χ is an increasing but rather complicated function of V and there is no way to solve for V_c analytically. However,

it was found [9] that the minimal value of V_c corresponds to the situation when the charge exchange frequency ω_R is of the same order as the eigenfrequency of the grain vibration ω.

Above the threshold voltage, the oscillation amplitude will increase exponentially until a balance between dissipated and absorbed energy is achieved and the system reaches a stable self-oscillating regime. The amplitude A of the self-oscillations will therefore be determined by the criterion $W(A) = Q(A)$.

The transition from the *static* to the *self-oscillating regime* can be associated with either *soft* or *hard* excitation of self-oscillations depending on the relation between the charge exchange frequency ω_R and eigenfrequency of grain oscillation ω_0 [9]. The soft excitation takes place if $\omega_R/\omega_0 > 2\sqrt{3}$. In this case the amplitude of the stable self-oscillation regime increases smoothly (with voltage increase) from zero at the transition voltage. In a case of hard excitation ($\omega_R/\omega_0 < 2\sqrt{3}$) the oscillation amplitude jumps to a finite value when the voltage exceeds V_c. It was also found [9] that the hard excitation is accompanied by a hysteretic behaviour of the current–voltage (I–V) characteristics.

In the fully developed self-oscillating regime the oscillating grain, sequentially moving electrons from one lead to the other, provides a 'shuttle mechanism' for charge, as shown in figure 1(b). In each cycle, $2n$ electrons are transferred, so the average contribution to the current from this shuttle mechanism is

$$I = 2enf, \qquad n = \left[\frac{CV}{e} + \frac{1}{2}\right], \tag{1}$$

where $f \equiv \omega_0/2\pi$ is the self-oscillation frequency and the square brackets indicate that the integer part should be taken. This current does not depend on the tunnelling rate ω_R. The reason is that when the charge jumps to or from a lead, the grain is so close that the tunnelling rate is large compared to the elastic vibration frequency. Hence the shuttle frequency—not the tunnelling rate—provides the 'bottleneck' for this process. We emphasize that the current due to this shuttle mechanism can be substantially larger than the conventional current via a fixed grain. This is the case when $\omega_0 \gg \omega_R$.

To support the qualitative arguments given above we have performed analytical and numerical analyses based on the simultaneous solution of Newton's equation for the motion of a grain's centre of mass and a master equation for the charge redistribution.

Two different approaches were developed. The first, presented in [8], gives the quantitative description of the shuttle instability for low tunnel barrier resistances when the rate of charge redistribution is so large (in comparison with the vibrational frequency) that the stochastic fluctuations in the grain charge during a single vibration period are unimportant. The second approach, describing the opposite limit of low-charge redistribution frequencies characteristic of high-resistance tunnel barriers, is presented in [9].

In both cases it was shown that the electromechanical instability discussed above has dramatic consequences for the current–voltage characteristics of a single-electron transistor configuration, as shown in figure 3. Even for a symmetric double junction, where no Coulomb staircase appears in conventional designs, we predict the shuttle mechanism for charge transport to manifest itself as a current jump at $V = V_c$ and as a Coulomb staircase as the voltage is further increased.

A more precise calculation along the line l sketched in figure 3 is shown in figure 4. The non-monotonic behaviour of the current along this line is due to competition between the two charge transfer mechanisms present in the system, the ordinary tunnel current and the mechanically mediated current $I_{mech}(x_0, t) = \delta(x(t) - x_0)\dot{x}(t)q(t)$ through some cross-section at x_0. We define the shuttle current as the time-averaged mechanical current through the plane located at $x_0 = 0$. This current, together with the tunnel current for the same cross-section, is shown in figure 4. As the damping in the system is reduced, the oscillation amplitude grows

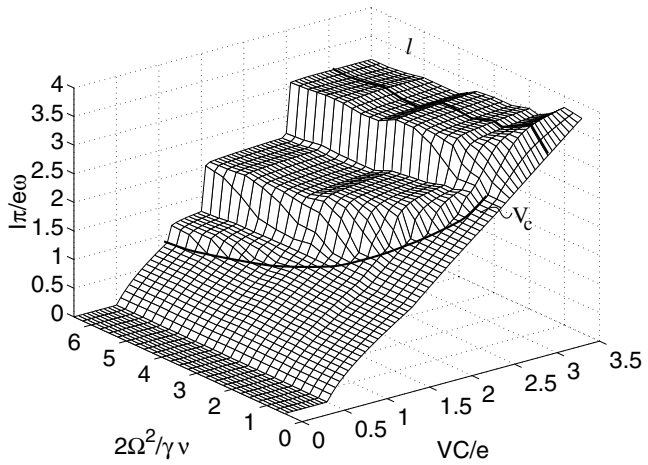

Figure 3. Current due to the shuttle mechanism through the composite Coulomb-blockade system of figure 1. The current is normalized to the eigenfrequency ω of elastic grain vibrations and plotted as a function of normalized bias voltage V and inverse damping rate γ^{-1}. With infinite damping, no grain oscillations occur and no Coulomb staircase can be seen. The critical voltage V_c required for the grain to start vibrating is indicated by a line. From [8]. © (1998) by the American Physical Society.

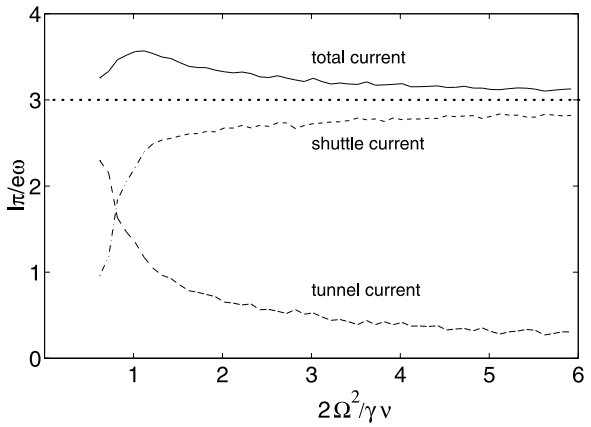

Figure 4. The cross-section along the line l in figure 3. The total time-averaged current consist of two parts, the shuttle current and the tunnelling current. The time-averaged shuttle current is the current transferred mechanically through the centre of the system, $\langle \delta(x(t))\dot{x}(t)q(t)\rangle$; the remaining part comes from ordinary tunnelling. As the inverse damping γ^{-1} increases, the shuttle current approaches the quantized value $I\pi/e\omega = 3$. The tunnel current is proportional to the fraction of the oscillation period spent in the middle region, $|x| < \lambda$. This fraction is inversely proportional to the oscillation amplitude and hence the tunnel current decreases as γ^{-1} increases. The fine structure in the results is due to numerical noise. From [8]. © (1998) by the American Physical Society.

and the shuttle current is enhanced while the ordinary tunnelling current is suppressed. In the limit of low damping, this leads to a quantization of the total current in terms of $2ef$.

2.1.3. Shuttling in dissipative nanostructures. From the above analysis it is clear that a large damping is detrimental for the development of the shuttle instability and, in the limit

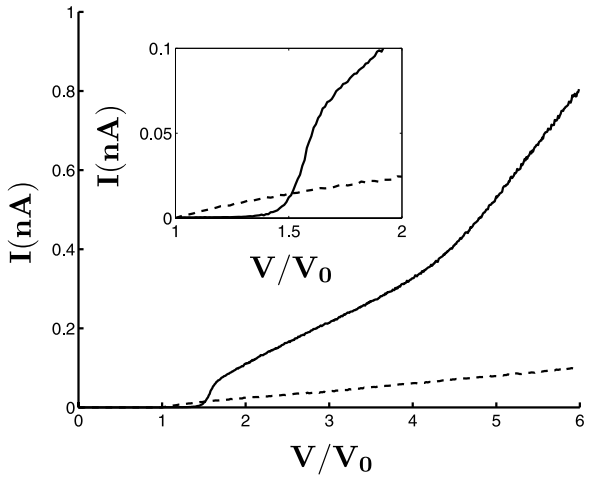

Figure 5. The solid curve shows the current–voltage characteristics obtained by a Monte Carlo simulation of the charge transport through a dissipation-dominated system. The calculated direct current is plotted as a function of the bias voltage V scaled by the Coulomb-blockade threshold voltage V_0, that applies if the movable grain is equally far from the two electrodes. The dashed curve displays the current through a static symmetric double junction for the same parameters. For voltages above the threshold voltage V_t, the current through the system increases drastically due to grain motion. The inset shows a magnification of the voltage interval around V_t. From [11]. © (2002) by the American Physical Society.

where $\gamma \gtrsim \omega_0$, elastic shuttling of the charge becomes impossible. The mechanical lability of the system, however, is still a dominating feature of the charge transport even in the limit of strong dissipation. The consequences of such a lability are addressed in [11]. There the elastic restoring force is assumed absent or much weaker than viscous damping forces. According to that model, charge transport through the NEM-SET is affected both by the Coulomb-blockade phenomenon and the mechanical motion of the cluster. These two phenomena are coupled, since the threshold voltage for electron tunnelling depends on the junction capacitances which, in turn, depend on the cluster position with respect to the leads. In general, the threshold voltage increases when the distance between the cluster and an electrode decreases.

To be specific, if a neutral cluster is located in its equilibrium position between the electrodes, no tunnelling takes place for a bias voltage V lower than some threshold value V_0. At $V > V_0$ the cluster can be charged due to tunnelling onto the cluster. At the same time, the electrical forces produce a mechanical displacement directed *from* the lead which has supplied the extra charge. After some time, the extra charge will leak to the nearest electrode, and the cluster becomes neutral again. An important question at this stage is whether an *extra* event of tunnelling to the nearest electrode can take place. The answer is not obvious, since the electrostatic tunnelling threshold in the last position is different from that at the initial point in the system's centre. Consequently, tunnelling to the nearest electrode, in principle, could be suppressed due to the Coulomb blockade. The analysis made in [11] has shown that at zero temperature there is an upper threshold voltage V_t below which the extra tunnelling event is not possible. In this case the cluster is almost trapped near the electrode and the conductance is not assisted by significant cluster displacements between the electrodes.

For voltages above the threshold, $V > V_t$, there is a possibility for another tunnelling event between the grain and the nearest lead to happen after the extra charge has tunnelled off the cluster. This event changes the sign of the net charge on the grain. In this case the cluster

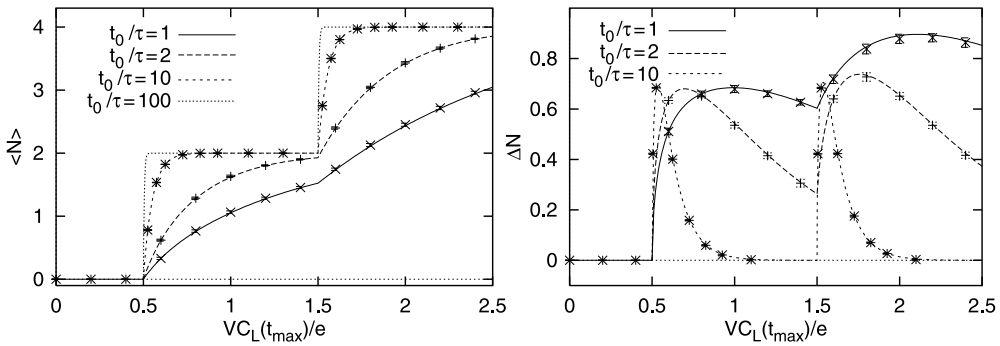

Figure 6. The average number of electrons transferred per period (left) and the root mean fluctuations (right) for $T = 0$. Coulomb blockade is clearly visible: up to a critical voltage ($VC_{\rm L}(t_{max})/e = \frac{1}{2}$), no electrons are transferred. From [12]. © (1999) EDP Sciences.

can be pushed by the Coulomb force towards the more distant electrode where the above-described process repeats itself. The conductance is now assisted by significant displacements of the grain, and this scenario is qualitatively similar to the shuttle vibrations in fully elastic electromechanical structures [8]. This process is also accompanied by a marked rise in the current through the system, as shown in figure 5.

2.1.4. Accuracy of a mechanical single-electron shuttle. Several mechanisms contribute to a deviation of the average current from the ideal shuttle value nef_0:

(i) 'Shunting' sequential electron tunnelling and cotunnelling through the grain, which leads to a direct current without any grain motion.
(ii) The length of time t_0 that the grain is in tunnelling contact with a lead at the trajectory turning point in relation to the charge relaxation time ω_R^{-1}. This relation determines whether the grain can be fully loaded during a single contact event.
(iii) Thermal fluctuations which lift the Coulomb-blockade-imposed limitation of the transferred charge being an integer.

The contribution of the shunting tunnelling seems to be much smaller than the current conveyed by a shuttling grain. Indeed, the former is limited by the *maximum* tunnel resistance, which is *exponentially large*. The second and third limitations on the accuracy of the shuttling current were considered in [12], where a master equation for the charge of the moving grain was analysed. In this approach the shuttling was mapped onto a sequence of contact events when charge transfer takes place. The results of analytical treatment of a simple model and of numerical treatment are shown in figures 6 and 7 taken from the paper [12]. In figure 6 the average number of electrons transferred per period, as well as the root mean fluctuations, are shown for $T = 0$. In this figure t_0 represents the effective time that the grain spends in contact with the leads, while τ denotes the time RC at the point of closest approach to the leads. Assuming that the grain is closest to the leads at a time t_{max}, one has $\tau = R(t_{max})C(t_{max})$. Thermal smearing of the single-electron shuttling is demonstrated in figure 7. It is clear that for $t_0 \gg \tau$ and $T = 0$ the Coulomb staircase is perfect. For increasing temperatures, the Coulomb staircase is washed out, leading to an ohmic behaviour for high temperatures.

2.1.5. Gate voltage control of the shuttle mechanics. The electromechanical coupling also dramatically changes the transistor effect in a NEM-SET as compared to an ordinary SET.

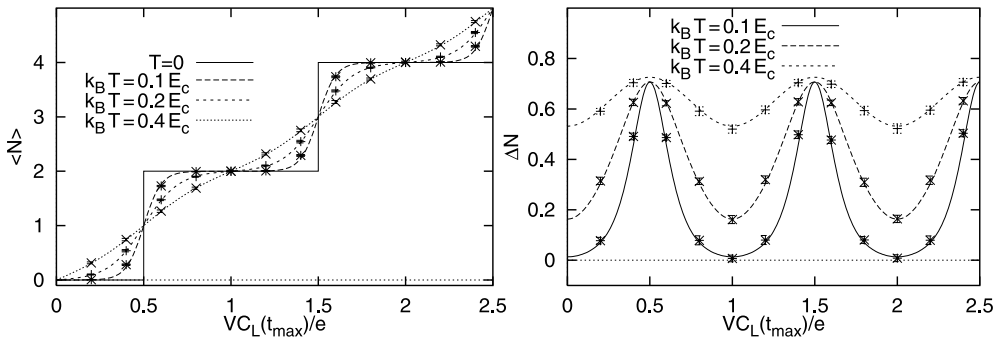

Figure 7. Thermal smearing of single-electron shuttling. The energy scale is given by $E_C = e^2/2C$. t_{max} is the instant when a particle is located at a turning point. From [12]. © (1999) EDP Sciences.

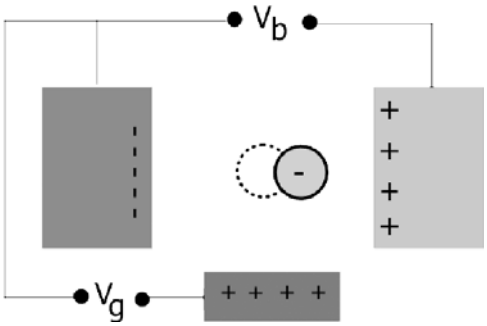

Figure 8. Schematic configuration of a nanoelectromechanical single electron transistor (NEM-SET).

We will discuss this problem following [13]. Let us assume that the tunnelling can take place only between the grain and the leads, while there is no tunnelling exchange with the gate. The gate voltage controls the equilibrium position of the grain with respect to the leads since it determines the extra charge of the grain. A schematic configuration of a relevant NEM-SET is sketched in figure 8. The picture shows a situation when the grain has a net negative charge. The net negative charging of the grain occurs at a certain relation between the bias, V_b, and the gate, V_g, voltages. The positively charged gate electrostatically induces a negative charge on the grain, which tends to be compensated by the tunnelling of positive charge from the right-hand lead[4]. Since the grain is shifted from the central position, the current through the device is exponentially small. An increase in the bias voltage decreases the total negative charge. At complete compensation the grain returns to the central position, restoring the tunnelling transport through the device. The 'phase diagram' in the V_g–V_b plane obtained in [13] is shown in figure 9. It is worth mentioning a *qualitative* difference of this 'butterfly' phase diagram from the conventional 'diamond' phase diagram of the conventional SET[5] where the mechanically blocked SET operation is absent.

2.1.6. Nanoparticle chains. We conclude this section concerning classical shuttling of electrons by considering theoretical work regarding nanoparticle chains [14]. Nanoparticle

[4] Here we assume that the tunnelling from the negatively charged remote electrode is exponentially suppressed.
[5] Diamond structure.

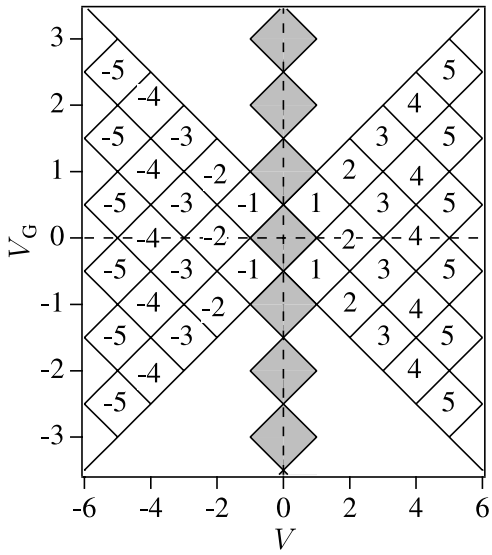

Figure 9. A diagram of the current I in the bias voltage–gate voltage plane (V and V_G, respectively) for symmetrically applied source–drain voltage. The shaded diamonds denote the voltage region where electron tunnelling is prohibited at $T = 0$. The white areas correspond to *mechanically suppressed* SET operation. From [13] © (2001) by the American Physical Society.

chains consist of small metal grains stabilized by ligands, with electronic transport occurring via tunnelling between the metal particles. Because of the relative softness of the ligand matrix, vibrations of the metal grains can significantly modify the electronic tunnelling rates. In the systems with several degrees of freedom, the electromechanical instability at special values of system parameters can lead to excitation of more than one mode. As a result, the mechanical motion becomes in general non-periodic with a possibility of a telegraph-like switching between the modes. A crossover from a periodic to a quasiperiodic motion, as well as telegraph-like switching between these regimes was demonstrated in [14, 15]. In that paper, electron shuttling through a system of two elastically and electrically coupled particles was numerically simulated, and a telegraph-like switching was observed at some value of the bias voltage.

2.2. Classical shuttling of electron waves

In this section we follow the considerations of [10]. There it is assumed that a vibrating grain has a single resonant level; both the position $x(t)$ of this level and the coupling of the grain to the leads, $T_{L,R}(t)$, are oscillatory functions of time—see figure 10. The effective Hamiltonian of the problem is defined as

$$H = \sum_{\alpha,k}(\epsilon_{\alpha k} - \mu_\alpha)a^\dagger_{\alpha k}a_{\alpha k} + \epsilon_d(t)c^\dagger c + \sum_{\alpha,k} T_\alpha(t)(a^\dagger_{\alpha k}c + c^\dagger a_{\alpha k}). \tag{2}$$

Here $T_{L,R} = \tau_{L,R}\exp\{\mp x(t)/2\lambda\}$ is the position-dependent tunnelling matrix element, $\epsilon_d(t) = \epsilon_0 - e\mathcal{E}x(t)$ is the energy level in the dot shifted due to the voltage-induced electric field $\mathcal{E}$, $a^\dagger_{\alpha k}$ creates an electron with momentum k in the corresponding lead, $\alpha = L, R$ is the lead index, $c^\dagger$ creates an electron in the dot. The first term in the Hamiltonian describes the electrons in the leads, the second corresponds to the movable quantum dot, and the last term describes tunnelling between the leads and the dot.

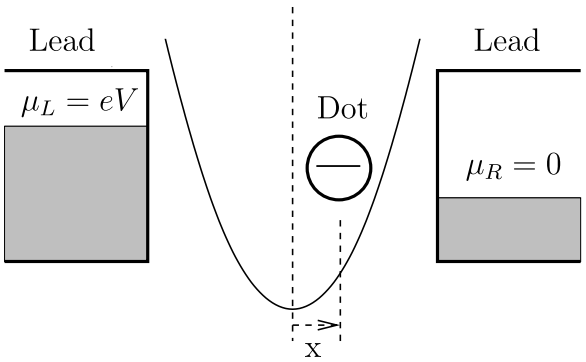

Figure 10. The model system consisting of a movable quantum dot placed between two leads. An effective elastic force acting on the dot from the leads is described by the parabolic potential. Only one single-electron state is available in the dot and the non-interacting electrons in each have a constant density of states. From [10]. © (2002) EDP Sciences.

The evolution of the electronic subsystem is determined by the Liouville–von Neumann equation for the statistical operator $\hat{\rho}(t)$:

$$\mathrm{i}\,\partial_t \hat{\rho}(t) = \hbar^{-1}[\hat{H}, \hat{\rho}(t)]_-, \tag{3}$$

while the centre-of-mass motion of the dot is governed by Newton's equation:

$$\ddot{x} + w_0^2 x = F/m. \tag{4}$$

Here $\omega_0 = \sqrt{k_0/m}$, m is the mass of the grain, k_0 is a constant characterizing the strength of the harmonic potential, $F(t) = -\operatorname{Tr}[\hat{\rho}(t)\,\partial\hat{H}/\partial x]$. The force F is computed from an exact solution of the tunnelling problem, which exists for arbitrary $T_\alpha(t)$ and $\epsilon_d(t)$. Using the Keldysh Green function approach [16] in the so-called wide-band approximation and following [17], one obtains the force F as

$$F(t) = \sum_\alpha g_\alpha \int \mathrm{d}\epsilon\; f_\alpha(\epsilon)\left\{e\mathcal{E}|B_\alpha(\epsilon,t)|^2 + \frac{(-1)^\alpha}{\lambda} T_\alpha(t)\,\mathrm{Re}[B_\alpha(\epsilon,t)]\right\}, \tag{5}$$

where

$$B_\alpha(\epsilon,t) = -\mathrm{i}\hbar^{-1}\int_{-\infty}^{t} \mathrm{d}t_1\; T_\alpha(t_1)\exp\left\{\mathrm{i}\hbar^{-1}\int_{t_1}^{t}\mathrm{d}t_2\left[\epsilon - \epsilon_d(t_2) + \mathrm{i}\frac{\Gamma(t_2)}{2}\right]\right\},$$

and $\Gamma(t) = 2\pi\sum_\alpha g_\alpha |T_\alpha(t)|^2$, g_α is the density of states in the corresponding lead, while $f_\alpha(\epsilon) = \{\exp[\beta(\epsilon-\mu_\alpha)]+1\}^{-1}$. The first item in the expression (5) for $F(t)$ is the electric force due to accumulated charge; the second one is the 'cohesive' force due to position-dependent hybridization of the electronic states of the grain and the leads. Equations (4) and (5) can be used to study stability of the equilibrium position of the cluster. By linearizing equation (4) with respect to the small displacement $\propto \mathrm{e}^{-\mathrm{i}\omega t}$ and by solving the proper equations of motion, one can obtain a *complex* vibration frequency. The mechanical instability can then be found from the criterion $\mathrm{Im}\,\omega \geqslant 0$. As shown in [10], the instability occurs if the driving voltage exceeds some critical value which for symmetrically applied voltage is $eV_c = 2(\epsilon_0 + \hbar\omega_0)$. It was also shown that in the limit of weak electromechanical coupling, when $\Gamma/(4m\omega_0^2\lambda^2)$, and $2e\mathcal{E}\lambda/\left(\sqrt{\hbar^2\omega_0^2+\Gamma^2}\right) \ll 1$, the instability develops into a limiting cycle. This is in contrast with the case for a classical shuttle, where stability of the system could be achieved only at finite mechanical dissipation. The reason for the difference is that in the present situation the dissipation is provided by coupling to electronic degrees of freedom. In the

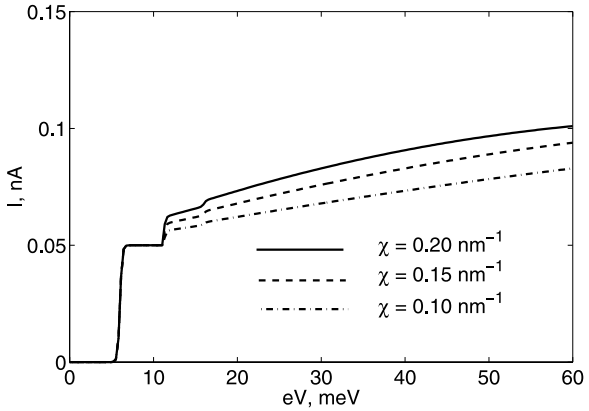

Figure 11. I–V curves for different values of the parameter χ which characterizes the strength of the electric field between the leads for a given voltage: $\hbar\omega_0 = 5$ meV, $T = 0.13$ meV, $\epsilon_0 = 6$ meV, and $\Gamma = 2.3$ μeV. The best fit to [7] is obtained for an asymmetric coupling to the leads; here we use $\Gamma_R/\Gamma_L = 9$. From [10]. © (2002) EDP Sciences.

classical treatment this dissipation mechanism has been disregarded, since phonon-assisted tunnelling was ignored. One can see a qualitative agreement between the experimentally observed $I(V)$ curve for a fullerene-based NEM-SET in figures 13 and 11 where results of the above calculation are presented. However, there are alternative interpretations of the experiment [7] (see [18, 19]), based on a quantum mechanical treatment of the mechanical motion. We will discuss these explanations below.

2.3. Charge transfer through a quantum oscillator

In the previous discussion we assumed that the mechanical degree of freedom was classical. However, the centre-of-mass displacement can be comparable with the quantum mechanical zero-point vibration amplitude, $x_0 = \sqrt{\hbar/m\omega_0}$. In this case electronic and mechanical degrees of freedom behave as coupled parts of a quantum system which should be described by quantum mechanics. The coupling between the subsystems occurs due to

(i) dependences of the electronic levels, charges, their images, and, consequently, electric forces on the mechanical degrees of freedom;
(ii) the dependence of the tunnelling barriers on the spatial system configuration.

In general, the charge transfer in the systems under consideration is assisted by excitation of vibrational degrees of freedom, which is similar to phonon-assisted tunnelling through nanostructures. However, in some cases the centre-of-mass mechanical mode turns out to be more strongly coupled to the charge transfer than other modes. In this case one can interpret centre-of-mass mode-assisted charge transfer as a *quantum shuttle* provided that the centre-of-mass motion is correlated with the time-dependent charge on the dot (see the definition of shuttle transport in the introduction). Several papers have addressed the charge transport through a quantum oscillator, and several models have been discussed. Some of these works are reviewed below.

Single-electron tunnelling through molecular structures under the influence of nanomechanical excitations has been considered by Boese and Schoeller [18]. The authors developed a quantum mechanical model of electron tunnelling through a vibrating molecule and applied it to the experiment [7]. Contrary to the situation described in sections 2.1, 2.2,

and [8, 10], it is assumed that the vibrational frequency is several orders of magnitude larger than the frequency associated with tunnelling effects. The system is described by an effective Hamiltonian involving local bosonic degrees of freedom of the molecule. One of the local modes can be interpreted as centre-of-mass motion. The quantum mechanical calculation leads to a set of horizontal plateaus in the I–V curve due to excitation of different vibrational modes. It is shown that in some regions of the parameters a negative differential resistance occurs. A similar calculation, but with a more detailed account of the dependence of the charge transfer matrix elements in the shuttle coordinate, was reported by McCarthy *et al* [19].

The papers [18] and [19] provide a qualitative explanation for the experiment [7]. This explanation is actually an alternative to that given in [10], where the centre-of-mass motion was treated classically. It is worth mentioning that the latter model predicts a finite slope of the I–V curve at large voltages, which is more similar to the experimental result.

A quantum oscillator consisting of a dot on springs flanked by two stationary dots attached to semi-infinite leads was considered by MacKinnon and Armour [20]. The authors concentrate on quantum aspects of the dot and electron motion. It is shown that the I–V characteristics of the model shuttle can largely be understood by analysing the eigenspectrum of the isolated system of three dots and the quantum oscillator. Tunnel coupling of the dot states, to each other and to the position of the oscillator, leads to repulsion of the eigenvalues and mixing of the eigenstates associated with states localized on individual dots. The mixed states consist of superpositions of the states associated with the individual dots and hence lead to delocalization of the electronic states between the dots. Analysis of the current which flows when the shuttle is weakly coupled to leads reveals strong resonances corresponding to the occurrence of the delocalized states. The current through the shuttle is found to depend sensitively on the amount by which the oscillator is damped, the strength of the couplings between the dots, and the background temperature. When the tunnelling length λ of the electrons is of order x_0, current far from the electronic resonance is dominated by electrons hopping on and off the central dot sequentially. As the authors state, then the oscillator can be regarded as shuttling electrons across the system, as has been discussed in section 2.1.

3. Experiments on electron shuttling

The first experimental realization of the shuttle instability resulting in a classical shuttle electron transfer was reported by Tuominen *et al* [6]. The experimental set-up is shown in figure 12. The measured current–voltage characteristics display distinctive jumps and hysteresis which reflect the influence of the vibrational environment (the metal beam in figure 12) on the shuttle dynamics.

Systems in which electron transport between two contacts is mediated by a vibrational mode of a self-assembled structure have also been investigated [7, 21]. The most striking example of such a system is the C_{60} single-electron transistor, fabricated by Park *et al* [7]. In this device, a single C_{60} molecule was deposited in a narrow gap between gold electrodes. The current flowing through the device was found to increase sharply whenever the applied voltage was sufficient to excite vibrations of the molecule about the minima of the van der Waals potential in which the molecule resides, or an internal mode of the molecule itself.

These transport measurements provided clear evidence for coupling between the centre-of-mass motion of the C_{60} molecules and single-electron hopping. This new conduction mechanism had not been observed previously in quantum dot studies. The coupling is manifested as quantized nanomechanical oscillations of the C_{60} molecule against the gold surface, with a frequency of about 1.2 THz. This value is in good agreement with a simple theoretical estimate based on van der Waals and electrostatic interactions between C_{60} molecules and gold electrodes. The observed current–voltage curves are shown in figure 13.

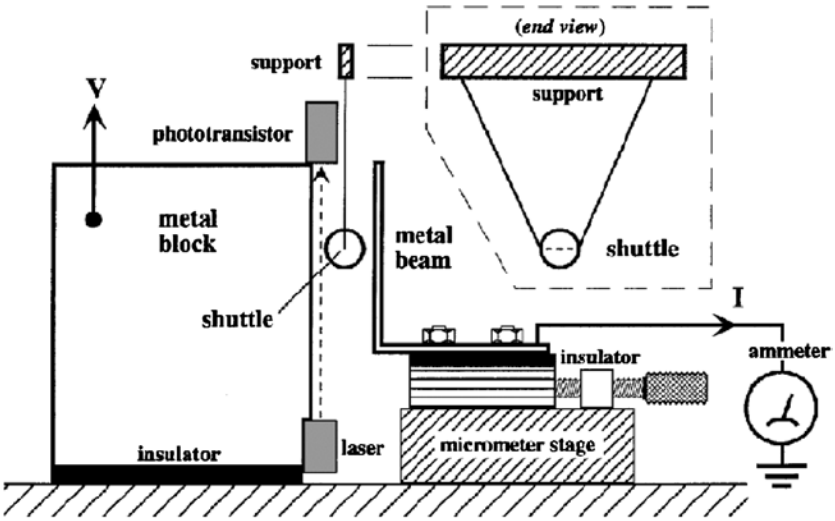

Figure 12. The experimental set-up. The block, shuttle, and beam are made of brass. The dimensions of the beam are 40 mm × 22 mm × 1.6 mm. The shuttle mass is 0.157 g, its radius 2.06 mm; the effective mass of the bending beam is 30 g, its fundamental vibrational frequency 210 Hz, and its quality factor 37. Measurements indicate the influence of another vibrational mode at 340 Hz. The micrometer is used to adjust the shuttle gap d. The natural pendulum frequency of the suspended shuttle is 2.5 Hz. From [6]. © (1999) by the American Physical Society.

The device fabricated by Park *et al* is an example of a molecular electronic device [22] in which electrical conduction occurs through single molecules connected to conventional leads. The junctions between molecular components and leads will be much more flexible than those in conventional solid-state nanostructures, and fluctuations in their width may modify the current characteristics significantly. Furthermore, vibrational modes of the molecular components themselves may play an important role in determining the transport properties [23].

An interesting possibility of a nanomechanical double-barrier tunnelling structure involving shuttling has been realized by Nagano *et al* [24, 25]. The system consists of a scanning vibrating probe/colloidal Au particles/vacuum/PtPd substrate; see figure 14. The colloidal particles act as Coulomb islands; due to probe vibration they are brought to motion. What is important is the phase shift between the probe vibrations and the alternating current in the system which allows one to single out the displacement current. The latter shows clear features of the Coulomb blockade. Comparison of the experimental results with theoretical calculation drove the authors to the conclusion that about 280 Au particles vibrate in accordance with each other.

An *externally driven* nanomechanical shuttle has been designed by Erbe *et al* [3, 4]. In these experiments a nanomechanical pendulum was fabricated on a Si-on-insulator substrate using electron and optical lithography, and a metallic island was placed on the clapper which could vibrate between the source and drain electrodes; see figure 15. The pendulum was excited by ac power by two gates on the left- and right-hand sides of the clapper. The observed tunnelling source–drain current was strongly dependent on the frequency of the exciting signal, having pronounced maxima at the frequencies of the mechanical modes. This fact signals a shuttling mechanism of electron transfer at typical shuttle frequencies of about 100 MHz. The measured average direct current at 4.2 K corresponded to 0.11 ± 0.001 electrons per cycle of mechanical motion. Theoretical analysis [12] and numerical simulations showed that a large

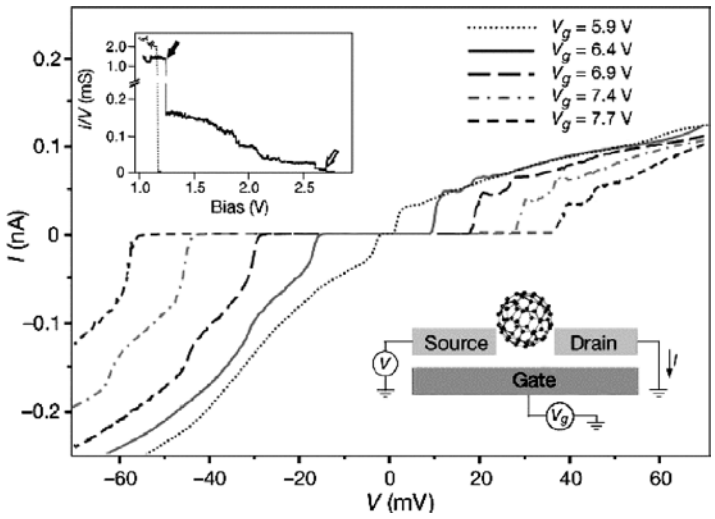

Figure 13. Current–voltage (I–V) curves obtained from a single-C_{60} transistor at $T = 1.5$ K. Five I–V curves taken at different gate voltages (V_g) are shown. Single-C_{60} transistors were prepared by first depositing a dilute toluene solution of C_{60} onto a pair of connected gold electrodes. A gap of 1 nm was then created using electromigration-induced breaking of the electrodes. Upper inset: a large bias was applied between the electrodes while the current through the connected electrode was monitored (solid curve). After the initial rapid decrease (solid arrow), the conductance stayed above ∼0.05 mS up to ∼2.0 V. This behaviour was observed for most single-C_{60} transistors, but it was not observed when no C_{60} solution was deposited (dotted curve). The bias voltage was increased until the conductance fell low enough to ensure that the current through the junction was in the tunnelling regime (open arrow). The low-bias measurements shown in the main panel were taken after the breaking procedure. Lower inset: an idealized diagram of a single-C_{60} transistor formed by this method. Reprinted by permission from *Nature* (from [7]). ©(2000) Macmillan Publishers Ltd.

proportion of the voltage also acts on the island. The authors of [3, 4] expect the resolution of the transport through the shuttle to also resolve the Coulomb blockade after minimizing the effects of the driving ac voltage. According to their estimates, Coulomb blockade should be observable below 600 mK. A very important modification of the set-up in figure 15 was recently presented by Scheible *et al* [5]. There, a silicon cantilever is part of a mechanical system of coupled resonators—a construction that makes it possible to drive the shuttle mechanically with a minimal destructive influence from the actuation dynamics on the shuttle itself. This is achieved by a clever design that minimizes the electrical coupling between the driving part of the device (either a magnetomotively driven, doubly clamped beam resonator, or a capacitively coupled, remote cantilever) and the driven part (the cantilever which carries the shuttle on its tip). Systems of the above-mentioned type can, in principle, be used for studies of shuttle transport through superconducting and magnetic systems.

Coupling of electron transport to mechanical degrees of freedom can lead to other interesting phenomena. In particular, Kubatkin *et al* [26] have observed a current-induced Jahn–Teller deformation of a Bi nanocluster. They have shown that such a transformation influences the electron transport through a change in the geometrical shape of the cluster.

4. Coherent transfer of Cooper pairs by a movable grain

In this section we study a superconducting weak link where the coupling between two bulk superconductors is due to Cooper pairs tunnelling through a small movable superconducting

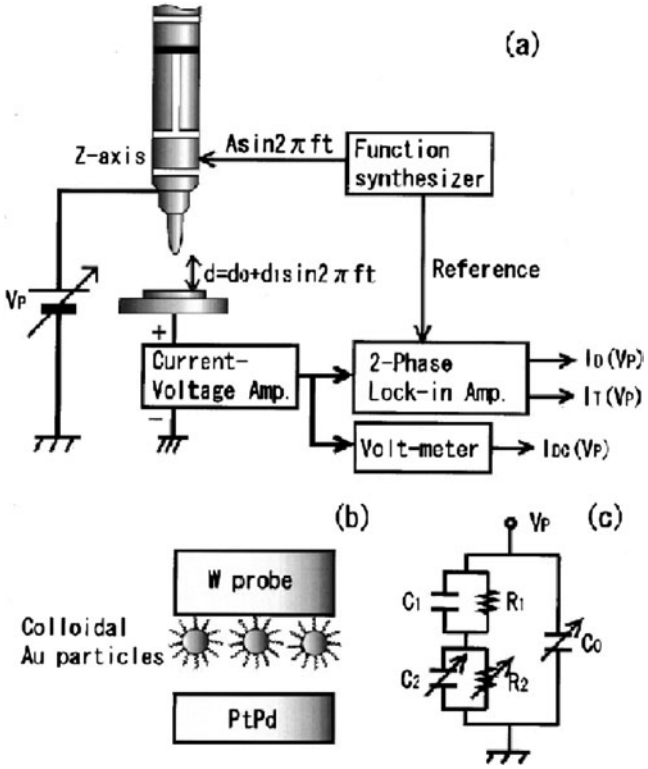

Figure 14. (a) The experimental arrangement of the tunnelling current and displacement current simultaneous measuring system. (b) A schematic image of nanomechanical double-barrier tunnelling structures with vibrating probe (W)/colloidal Au particles (diameter 8 nm)/vacuum/PtPd substrates. (c) The equivalent circuit of a two-junction system. C_1 and R_1 mean the capacitance and tunnelling resistance between a Au particle and a PtPd substrate, and C_2 and R_2 are those between a Au particle and a tungsten probe, respectively. C_0 is the capacitance between the tungsten probe and PtPd substrate. From [25]. © (2002) American Institute of Physics.

grain. The system is depicted in figure 16. We begin this section by looking at the requirements one has to impose on the system for the analysis below to be valid. Then we briefly review the 'parity effect' and the single-Cooper-pair box in section 4.2. Following this, in section 4.3, we consider the two basic processes involved in shuttling of Cooper pairs:

(i) scattering of a single grain with a lead, thereby creating entanglement; and
(ii) free motion of a grain whose charge state is a quantum mechanical superposition.

Two possible experimental configurations can be imagined for the system in figure 16:

(i) The pair of remote superconductors might be coupled by an external superconducting circuit, forming a loop. In this case the superconducting phase difference is a given number (and is for example determined by a magnetic flux through the loop). Shuttling of Cooper pairs is in this case a mechanism allowing for supercurrent flow through the loop. This scenario is analysed in section 4.4.
(ii) A qualitatively different situation is when the two leads are disconnected from each other. Cooper-pair exchange between two remote and isolated superconductors (leads) is then allowed only through tunnelling via the single-Cooper-pair box, performing oscillatory

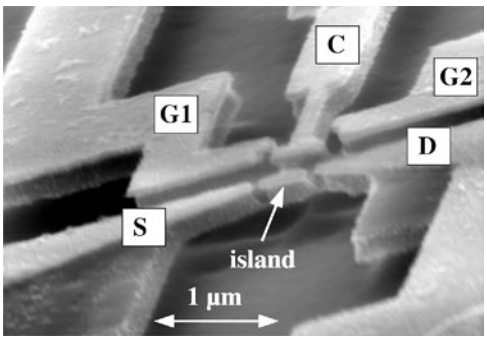

Figure 15. An electron micrograph of the quantum bell. The pendulum is clamped on the upper side of the structure. It can be set into motion by an ac power, which is applied to the gates on the left- and right-hand sides (G1 and G2) of the clapper (C). Electron transport is then observed from the source (S) to the drain (D) through the island on top of the clapper. The island is electrically isolated from the rest of the clapper which is grounded. From [3]. © (2001) by the American Physical Society.

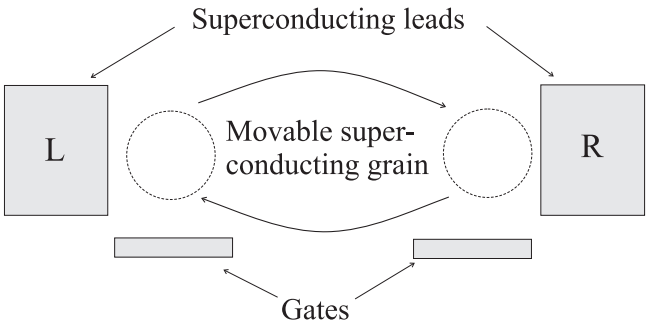

Figure 16. A superconducting shuttle junction. Two superconducting leads are placed too far away from each other to allow direct tunnelling between them. Using a movable grain they may still exchange Cooper pairs indirectly via lead–grain tunnelling. If the gates are appropriately biased, a single-Cooper-pair box situation occurs close to either lead allowing a coherent superposition of two different charge states on the grain. Hence, for a grain making repeated alternate contacts with the leads, a coherent exchange of Cooper pairs between them is possible.

motion between leads. In this case the relevant question is whether or not phase coherence between the leads can be established. This situation is considered in section 4.5.

4.1. Requirements for shuttling of Cooper pairs

The main question that we will focus on is how mechanical vibration of the cluster affects coherent tunnelling of Cooper pairs. To cast the question in a more dramatic form: could one have coupling between remote superconductors mediated mechanically through inter-lead transportation of Cooper pairs, performed by a small movable superconductor? The positive answer to this question which will be given here was partly presented in [27] and [28]. This follows from the possibility of preserving phase coherence of Cooper pairs despite the non-stationary and non-equilibrium dynamics of the electronic system originating from a time-dependent displacement of a small superconducting mediator. Such a possibility occurs if only a few electronic degrees of freedom are involved in the quantum dynamics. The latter is

guaranteed if two conditions are fulfilled:

(i) ω_0, the frequency of vibrations is much smaller than the superconducting gap frequency $\Delta/\hbar$.
(ii) The charging energy E_C is much larger than the superconducting coupling energy E_J and the thermal energy $k_B T$.

Here E_J is the maximal Josephson energy characterizing the superconducting coupling between the grain and the leads. Condition (i) prevents the creation of elementary electronic excitations due to the grain motion and therefore guarantees the disconnection of the system evolution from contributions relating to the continuous spectrum of quasiparticles on the superconductors. Condition (ii) guarantees a Coulomb blockade for Cooper-pair tunnelling, preventing a significant charge fluctuation on the dot. The appearance of such fluctuations corresponds to the existence of a large number of channels for the Cooper-pair transportation and results in strong decoherence due to destructive interference between these different channels. In what follows we will consider conditions (i) and (ii) as being fulfilled.

4.2. The parity effect and the single-Cooper-pair box

The ground state energy of a superconducting grain depends in an essential way on the number of electrons on it. Two contributions to such a dependence are given by the electrostatic Coulomb energy $E_C(N)$ connected with the extra charge accumulated on the superconducting grain and by the so-called parity term Δ_N [29–31]. The latter originates from the fact that only an even number of electrons can form a BCS ground state of a superconductor (which is a condensate of paired electrons) and therefore in the case of an odd number of electrons N one unpaired electron should occupy one of the quasiparticle states. The energy cost of occupying a quasiparticle state, which is equal to the superconducting gap Δ, brings a new scale to bear on the number of electrons that a small superconducting grain can hold. Taking the above into account, one presents the ground state energy $E_0(N)$ in the form (see [31])

$$E_0(N) = E_C(N - \alpha V_g)^2 + \Delta_N, \qquad \Delta_N = \begin{cases} 0 & \text{even } N \\ \Delta & \text{odd } N. \end{cases} \tag{6}$$

One can see from (6) that if $\Delta > E_C$ only an even number of electrons can be accumulated in the ground state of the superconducting grain. Moreover, for special values of the gate voltage V_g, such as $\alpha V_g = 2n + 1$, a degeneracy of the ground state occurs with respect to changing the total number of electrons by one single Cooper pair. An energy diagram illustrating this case is presented in figure 17. The occurrence of such a degeneracy brings about an important opportunity to create a quantum hybrid state at low temperatures which will be a coherent mixture of two ground states, differing by a single Cooper pair:

$$|\Psi\rangle = \gamma_1|n\rangle + \gamma_2|n+1\rangle. \tag{7}$$

An example of a system where this is possible is the so-called single-Cooper-pair box [30]. The possibility of creating a single-Cooper-pair box experimentally was demonstrated by Nakamura *et al* [32] and was recently confirmed by Devoret *et al* [33]. The idea of the experiment is presented in figure 18 where the superconducting dot is shown to be in tunnelling contact with a bulk superconductor. A gate electrode is responsible for lifting the Coulomb blockade of Cooper-pair tunnelling (by creating the ground state degeneracy discussed above). This allows the delocalization of a single Cooper pair between two superconductors. Such a hybridization results in a certain charge transfer between the bulk superconductor and the grain.

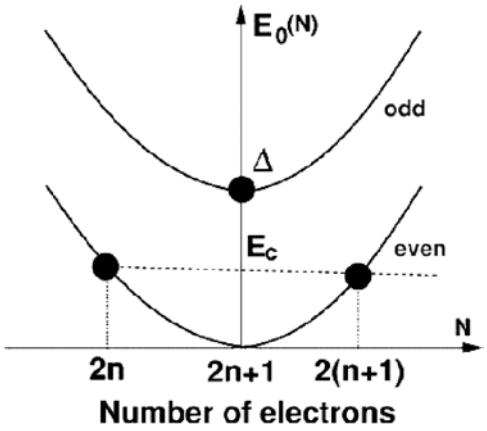

Figure 17. The energy diagram for the ground state of a superconducting grain with respect to charge for the case $\Delta > E_C$. For a certain bias voltage $\alpha V_g = 2n + 1$ (see equation (6)), ground states differing by only one single Cooper pair become degenerate.

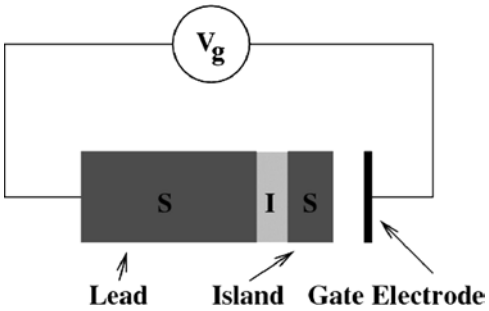

Figure 18. A schematic diagram of a single-Cooper-pair box. An island of superconducting material is connected to a larger superconducting lead via a weak link. This allows coherent tunnelling of Cooper pairs between them. For a nanoscale system, such quantum fluctuations of the charge on the island are generally suppressed due to the strong charging energy associated with a small grain capacitance. However, by appropriate biasing of the gate electrode it is possible to make the two states $|n\rangle$ and $|n+1\rangle$, differing by one Cooper pair, have the same energy (degeneracy of the ground state). This allows the creation of a hybrid state $|\Psi\rangle = \gamma_1|n\rangle + \gamma_2|n+1\rangle$.

4.3. Basic principles

The idea of shuttling of Cooper pairs is just an extension of the single-Cooper-pair box experiments presented in the last section. Essentially, to shuttle Cooper pairs, one uses the hybridization for coherent loading (unloading) of electrical charge to (from) a movable single-Cooper-pair box, performing a transportation of the loaded charge between remote superconductors. The necessary set-up should consist of the two above-mentioned configurations arranged in the vicinity of each lead as shown in figure 16. The superconducting grain performs periodic motion between the superconductors and the two gate electrodes ensure the lifting of the Coulomb blockade of Cooper-pair tunnelling at turning points in the vicinity of each of the superconducting electrodes.

4.3.1. Scattering and free motion. To illustrate the process, consider first the simple case when an initially uncharged grain, $n = 0$, arrives into contact with the left-hand lead. Before

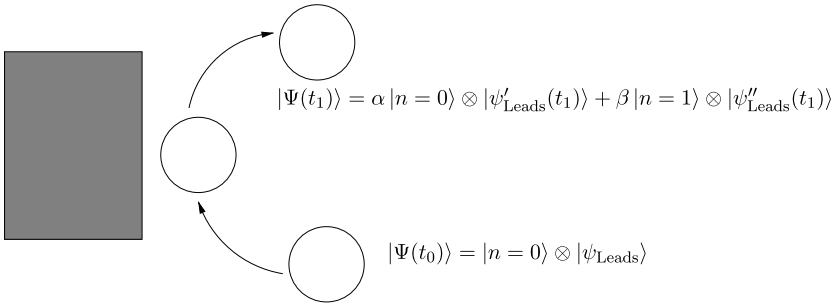

Figure 19. A grain initially carrying zero excess Cooper pairs scatters with the left-hand lead. After the scattering the state of the grain will be a superposition of zero and one extra Cooper pairs. In the process, the grain becomes entangled with the leads.

contact the state of the system is then

$$|\Psi(t_0)\rangle = |n=0\rangle \otimes |\psi_{\rm Leads}\rangle,$$

where $|\psi_{\rm Leads}\rangle$ is the state of the leads. During the time spent in tunnelling contact with the lead, the number of Cooper pairs on the grain may change. When the grain ceases to be in contact with the lead, the general state of the system is thus

$$|\Psi(t_1)\rangle = \alpha|n=0\rangle \otimes |\psi'_{\rm Leads}(t_1)\rangle + \beta|n=1\rangle \otimes |\psi''_{\rm Leads}(t_1)\rangle.$$

This process is depicted in figure 19. The coefficients α and β are complex and will depend both on the time spent in contact with the lead and on the initial state $|\psi_{\rm Leads}\rangle$. It is to be noted here that, in general, the grain will become entangled with the leads.

As the grain traverses the region between the leads, there is no tunnelling and the amplitudes $|\alpha|$ and $|\beta|$ will remain constant. However, the relative phase between them may change. Thus, when the grain arrives at the right-hand lead at a time t_2, the state of the system will have acquired an additional phase labelled χ_+:

$$|\Psi(t_2)\rangle = \alpha|0\rangle \otimes |\psi'_{\rm Leads}(t_2)\rangle + {\rm e}^{-{\rm i}\chi_+}\beta|1\rangle \otimes |\psi''_{\rm Leads}(t_2)\rangle.$$

As the grain comes into contact with the right-hand lead, charge exchange is again possible and the coefficients α and β will change. Then, in the same fashion as during the motion from left to right, the only effect on the state as the grain moves towards the left lead again is the acquiring of another relative phase denoted by χ_-. The whole process is schematically depicted in figure 20.

Both scattering events and 'free motion' are thus characterized by quantum phases accumulated by the system, which we call here the Josephson phase, ϑ, and the electrostatic phase, $\chi_\pm$:

$$\vartheta = \hbar^{-1}\int {\rm d}t\; E_J(t). \tag{8}$$

$$\chi_\pm = ({\rm i}/\hbar)\int {\rm d}t\;\delta E_c[x(t)] \tag{9}$$

4.3.2. The Hamiltonian. Under the condition that the grain position x varies adiabatically, no quasiparticle degrees of freedom are involved and one considers only the quantum dynamics of the coupled ground states on each of the superconductors. The corresponding Hamiltonian

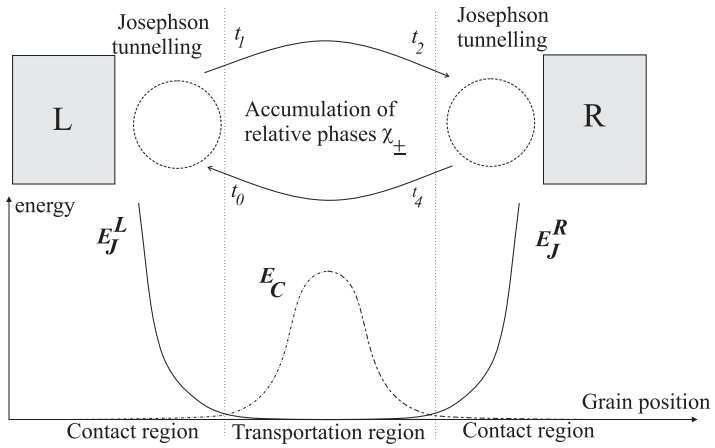

Figure 20. Illustration of the charge transport process. The island moves periodically between the leads. Close to each turning point, lead–grain tunnelling takes place. At these points the states with net charge 0 and $2e$ are degenerate. As the grain is moved out of contact, the tunnelling is exponentially suppressed, while the degeneracy may be lifted. This leads to the accumulation of electrostatic phases $\chi_{\pm}$.

is expressed through the operator $\hat{n}$ of the number of Cooper pairs on the grain and the phase operators of the leads, $\hat{\Phi}_{L,R}$:

$$H(x(t)) = -\tfrac{1}{2}\sum_{s=L,R} E_J^s(x(t))(\mathrm{e}^{\mathrm{i}\hat{\Phi}_s}|1\rangle\langle 0| + \mathrm{h.c.}) + \delta E_C(x(t))\hat{n}. \tag{10}$$

The operator $|0\rangle\langle 1|$ changes the (net) charge on the grain from zero to one extra Cooper pair. This Hamiltonian represents a standard approach to the description of superconducting weak links [34]. However, an essential specific feature is the dependence of the difference in charging energy δE_C and the coupling energies E_J on the position of the superconducting grain x,

$$E_J^{L,R}(x) = E_0 \exp(-\delta x_{L,R}/\lambda),$$

where $\delta x_{L,R}$ is the distance between the grain and the respective lead. Since the displacement x is a given function of time, this quantum problem is a non-stationary one.

4.4. Transferring Cooper pairs between coupled leads

When the leads are completely connected, i.e. they are simply different parts of the same superconductor, there is, due to charge conservation, a one-to-one correspondence between the number of pairs on the conductor and the number of pairs n on the island. One may in this case assume the leads to be in states with definite phases:

$$|\psi_{\mathrm{Leads}}\rangle = |\Phi_L\rangle \otimes |\Phi_R\rangle.$$

The effect of this is to replace the operators $\mathrm{e}^{\pm\mathrm{i}\hat{\Phi}_{L,R}}$ in the Hamiltonian above with c-numbers, making it a two-level system. This leaves us with a reduced Hamiltonian where the phases $\Phi_{L,R}$ enter only as parameters:

$$H_{red}(x(t), \Phi_L, \Phi_R) \equiv \langle\Phi_L|\langle\Phi_R|H(x(t))|\Phi_R\rangle|\Phi_L\rangle. \tag{11}$$

The dynamics of the system is described by the Liouville–von Neumann equation for the density matrix $\hat{\rho}$ [27]:

$$\mathrm{d}\hat{\rho}/\mathrm{d}t = -\mathrm{i}\hbar^{-1}[H_{red}, \hat{\rho}] - \nu(t)[\hat{\rho} - \hat{\rho}_0(t)]. \tag{12}$$

Since we are not interested here in transient processes, connected with the initial switching on of the mechanical motion, solutions which do not depend on any initial conditions will be focused upon in our analysis. To prevent any memory of initial conditions, one needs to include a dissipation term (the last term on the right-hand side of (12)) in the dynamics. If this dissipation is weak enough it does not affect the system dynamics on a timescale comparable to the period of vibrations. However, on a timescale longer than the period of rotation such relaxation causes a solution to (12) to be independent of any initial conditions. We choose the simplest possible form for relaxation (the τ-approximation) with ρ_0 being an equilibrium density matrix for the system described by Hamiltonian H. Relaxation is due to quasiparticle exchange with the leads and depends on the tunnelling transparencies

$$\nu(x) = \nu_0 \exp(-\delta x/\lambda). \tag{13}$$

The Cooper-pair exchange, being an exponential function of the grain position, is mainly localized in the vicinity of the turning points. In this region the Coulomb blockade of the Cooper-pair tunnelling is suppressed and can be neglected while considering the dynamics of the formation (or transformation) of the single-Cooper-pair hybrid; see equation (7). In contrast to this, the dynamics of the system in the time intervals when the grain is far away from the superconducting leads is not significantly affected by Cooper-pair tunnelling and essentially depends on the electrostatic energy $\delta E_C = E_C(n+1) - E_C(n)$ appearing due to the lifting of the Coulomb degeneracy in the regions far from the turning points. This circumstance allows the simplification of the analysis and consideration of the quantum evolution of the system as a sequence of scattering events (taking place due to tunnelling of Cooper pairs in the vicinity of the turning points) which are separated by intervals of 'free motion' of the system, where tunnelling coupling between the grain and leads is neglected. A schematic picture of the above regimes of evolution is presented in figure 20.

In the limit $\nu_0 \to 0$ direct calculations give the following simple expression for the average current [27] (for details of the derivation see also [35, 36]):

$$\bar{I} = 2ef \frac{\cos\vartheta \sin^3\vartheta \sin\Phi(\cos\chi + \cos\Phi)}{1 - (\cos^2\vartheta \cos\chi - \sin^2\vartheta \cos\Phi)^2}. \tag{14}$$

Here, $\Phi = (\Phi_R - \Phi_L) + (\chi_+ - \chi_-)$ and $\chi = \chi_+ + \chi_-$. The following features of equation (14) should be mentioned:

(i) The mechanically assisted supercurrent is an oscillatory function of the phase differences of the superconducting leads, similarly to the cases for other types of superconducting weak link.

(ii) The current can be electrostatically controlled if an asymmetrical (χ_+ is not equal to χ_-) phase accumulation is provided by an external electric field varying in tandem with the grain rotation. The same effect appears if the grain trajectory embeds a finite magnetic flux. Then χ is proportional to the flux given in units of the superconducting flux quantum.

(iii) Depending on the value of the electrostatic phase χ, one can have any direction of the supercurrent flow at a given superconducting phase difference. Also a non-zero supercurrent at $\Phi_L - \Phi_R = 0$ is possible, in contrast to the case for ordinary superconducting weak links.

(iv) The supercurrent is a non-monotonic function of the Josephson coupling strength ϑ. This fact reflects the well known Rabi oscillations in the population of quantum states with different numbers of Cooper pairs when a single-Cooper-pair box is formed due to sudden switching of pairs tunnelling at the turning points of the trajectory.

In the weak-coupling limit the current is proportional to the third power of the maximal Josephson coupling strength. One needs to stress that this strength might be several orders

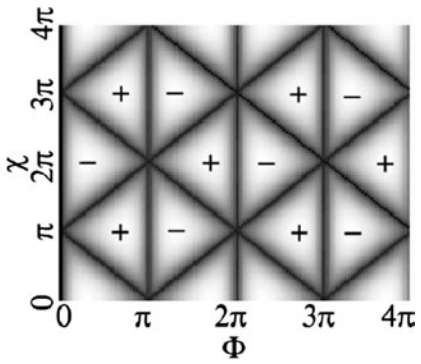

Figure 21. The magnitude of the current $\overline{I}$ in equation (14) in units of $I_0 = 2ef$ as a function of the phases Φ and χ. Regions in black correspond to no current and regions in white to $|\overline{I}/I_0| = 0.5$. The direction of the current is indicated in the figure by the signs $\pm$. To best show the triangular structure of the current, the contact time has been chosen to be $\vartheta = \pi/3$. I_0 contains only the fundamental frequency of the grain's motion and the Cooper-pair charge.

of magnitude larger than that corresponding to the real spatial separation between the superconducting leads. Cooper-pair transportation serves as an alternative to direct Cooper-pair tunnelling between the leads, thereby providing a mechanism for supercurrent flow between remote superconductors. In figure 21 a diagram of the supercurrent as a function of both superconducting and electrostatic phases is presented. Signs + and − represent the direction of the supercurrent while the black lines correspond to configurations with a zero value of the current.

4.5. Shuttling Cooper pairs between disconnected leads

We are now turning to the question of whether or not the superconducting coupling between remote and isolated superconductors can be established by mechanical shuttling of Cooper pairs between them [28]. Here we are interested in the situation when at an initial moment of time the shuttle is absent and no superconducting phases can be introduced on the leads (due to large quantum fluctuations of the phases on conductors with a fixed number of Cooper pairs). At times t bigger than zero, a superconducting grain between the leads starts to rotate, and the number of Cooper pairs on each lead is no longer conserved. The moving single-Cooper-pair box provides an exchange of Cooper pairs between the leads. We are interested to know whether this exchange is able to establish superconducting phase coherence between the leads.

In the case with strongly coupled leads the limitation that the grain could carry only zero or one excess Cooper pair reduced the problem to a two-state problem. Since the problem was essentially a two-conductor problem (grain + one lead), only this variable was needed to determine the state of the system. For the case with decoupled leads, one has to retain the operator nature of $\hat{\Phi}_{L,R}$ in the Hamiltonian (10). The dimensionality of the Hilbert space depends on the maximum number of Cooper pairs that can be accommodated on the leads. The factors that set a limit to this number are the capacitances of the leads, which are not present in the Hamiltonian (10). Instead of including these charging energy terms, another approach was been used in [28]. The Hilbert space was there reduced in such a way that each lead can only accommodate a maximum (minimum) of $\pm N$ extra Cooper pairs.

The time evolution of the system is determined by the Liouville–von Neumann equation for the density matrix. If the total number of particles in the system is conserved and one

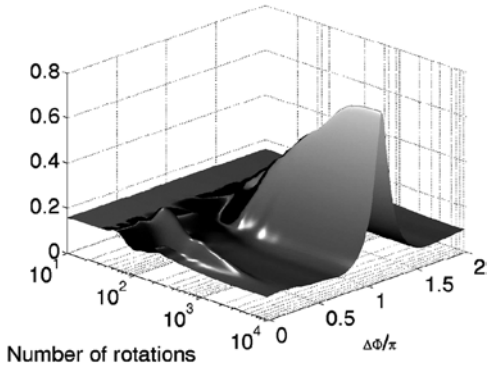

Figure 22. The probability for finding a phase difference $\Delta\Phi$ between the leads as a function of the number of grain rotations. From [28]. © (2003) by the American Physical Society.

assumes the whole system to be charge neutral, the state of the system can be written in terms of the state of the grain and one of the leads. For instance, the density matrix can be written as

$$\rho(t) = \sum_{\eta,\sigma=0,1} \sum_{N_L,N_L'=-N}^{N} \rho^{\eta\sigma}_{N_L N_L'}(t) \underbrace{|\eta\rangle\langle\sigma|}_{\text{grain}} \otimes \underbrace{|N_L\rangle\langle N_L'|}_{\text{left lead}} \otimes \underbrace{|-N_L-\eta\rangle\langle -N_L'-\sigma|}_{\text{right lead}}. \tag{15}$$

Here, which part of the system the various operators belong to has been explicitly indicated. The simple relaxation time approximation used for the case with connected leads cannot be used in this case. That approximation assumed the leads to be in BCS states with definite phases towards which the phase of the grain relaxed. Instead, to account for loss of initial conditions, the influence of the fluctuations of the gate potential on the island charge has been accounted for. The fluctuations are modelled by a harmonic oscillator bath with a spectral density determined by the impedance of the gate circuit. Hence, the density matrix in equation (15) is the reduced density matrix obtained after tracing out the bath degrees of freedom.

Denoting the phase difference between the leads by $\Delta\Phi \equiv \Phi_R - \Phi_L$ and the phase difference between the right-hand lead and the grain by $\Delta\phi \equiv \Phi_R - \phi_{\text{grain}}$, phase difference states

$$|\Delta\Phi, \Delta\phi\rangle \equiv \frac{1}{2\pi} \sum_n \sum_{N_L} \mathrm{e}^{-\mathrm{i}N_L\,\Delta\Phi} \mathrm{e}^{-\mathrm{i}n\,\Delta\phi} |n\rangle |N_L\rangle |-N_L-n\rangle$$

are introduced. The probability for finding a certain phase difference between the leads is then obtained from the reduced distribution function

$$f(\Delta\Phi) \equiv \int_0^{2\pi} \mathrm{d}(\Delta\phi) \langle \Delta\Phi, \Delta\phi|\rho|\Delta\Phi, \Delta\phi\rangle = \frac{1}{2\pi} \sum_{N_L,N_L'} \sum_{\eta} \mathrm{e}^{-\mathrm{i}(N_L'-N_L)\,\Delta\Phi} \rho^{\eta\eta}_{N_L N_L'}.$$

This is the function which has been plotted on the z-axis in figure 22. At the initial stage of the simulation the system was in a state with a definite charge on each conductor. This means that the phase distribution is initially completely flat. However, as the grain rotates the distribution is altered and eventually becomes peaked around a definite value of $\Delta\Phi$ uniquely determined by the system parameters. The width of the final peak depends on the maximum number of excess Cooper pairs that can be accommodated on the leads.

The phase difference built up due to the shuttle junction will determine the current through an ordinary junction connecting the leads if the latter is weak. In figure 23 this current is shown as a function of the dynamical phases for fixed ϑ (contact time). Here an auxiliary, weak, probe

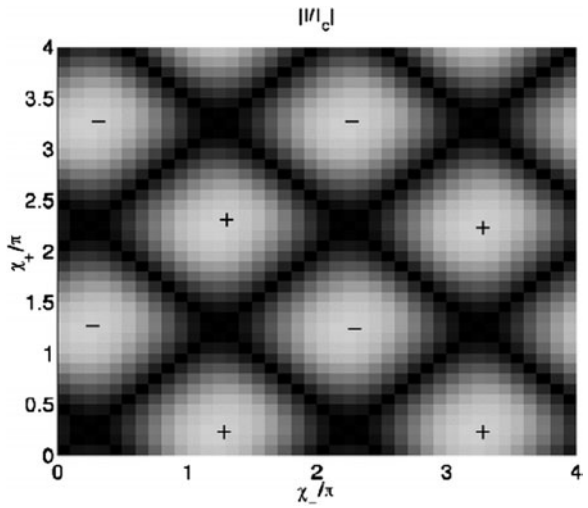

Figure 23. Current through a probe Josephson junction connected between the leads after many rotations. Bright areas correspond to large current while black ones correspond to zero current. The signs indicate the direction of the current. From [28]. © (2003) by the American Physical Society.

Josephson junction is assumed to be connected after a large number of rotations. The current is given by the usual Josephson relation weighted over the phase distribution $f(\Delta\Phi)$:

$$I = I_c \int_0^{2\pi} \mathrm{d}(\Delta\Phi) \sin(\Delta\Phi) f(\Delta\Phi),$$

where I_c is the critical current of the probe junction. The direction of the current is indicated by the signs in the graph. Black areas correspond to no current.

In conclusion, phase coherence can be established by mechanical transfer of Cooper pairs and this mechanism can also carry a non-dissipative current.

5. Discussion and conclusions

When designing nanometre-sized devices one inevitably faces Coulomb correlations that affect the electron transport. The most peculiar feature of such correlations is a single-electron mode of operation which determines the transport properties of many interesting nanodevices. Furthermore, in nanosystems electric charges produce not only large potential differences, but also large mechanical forces which can be comparable with atomic forces. These forces tend to produce mechanical displacements which, in turn, lead to a feedback to the distribution of electric charges. As result, coupling of electrical and mechanical degrees of freedom is a hallmark of nanodevices. The aim of this review is to demonstrate one fundamental manifestation of such coupled motion—the *shuttle* transfer of the charge due to electrons being carried by a movable part of the nanosystem. Shuttling of charge can either occur due to an intrinsic instability or be driven by an external ac source. From an 'applied' point of view, the role of shuttling can be either positive or negative. Indeed, it can hinder a proper operation of a single-electron transistor at the nanometre scale. On the other hand, an intended periodic mechanical motion resulting from the instability can be used to create building blocks for new applications. In particular, major new possibilities for generators and sensors at the nanometre scale appear.

As we have tried to show, the research area centred around the shuttle instability phenomenon involves several new principles and possibilities. Thus, there exists a rich physical picture containing both coherent and incoherent electron transport facilitated by either classical or quantum mechanical motion. In particular, one can expect very interesting physics regarding the coherent shuttling of Cooper pairs between superconductors which leads to an extension of the Josephson effect to relatively large distances, as well as to the creation of quantum coherence between remote objects by movable superconducting grains. This system, if realized experimentally, would allow for the determination of the decoherence rate of the superconducting devices due to their interaction with the environment.

One can imagine several concrete systems where electromechanical coupling is very important. Among them are nanoclusters and single molecules which can vibrate between the leads, metal–organic composites showing pronounced heteroelastic properties, colloidal particles, etc. A possibility of a similar physical picture involving coupling of *magnetic* and mechanical degrees of freedom has also been considered [37]. In the latter case the coupling is due to exchange forces, and it can lead to shuttling of magnetization.

There are a few experiments where electromechanical coupling has been observed, and some evidence in favour of single-electron shuttling was presented. The complete experimental proof of the single-electron shuttle instability remains a challenging problem. To solve this problem in a convincing way it seems to be a good idea to study anomalous structures of the Coulomb blockade in nanomechanical structures with and without gates, as well as to detect the periodic alternating current.

To summarize, movable nanoclusters can serve as new weak links between various normal, superconductor, and magnetic systems.

Acknowledgments

We acknowledge financial support from the Swedish Research Council (RIS, LIG) and the Swedish Foundation for Strategic Research though the programme QDNS (AI). The work was also supported by the US Department of Energy Office of Science through contract No W-31-109-ENG-38.

Note added in proof. The role of decoherence in a Cooper pair shuttle was recently analysed by Romito *et al* [38]. Both the average Josephson current and noises were considered. It has been shown that decoherence can either suppress or enhance the critical current.

References

[1] Andres R P *et al* 1996 *Science* **272** 1323
[2] Giaver I and Zeller H R 1968 *Phys. Rev. Lett.* **20** 1504
Shekhter R I 1973 *Sov. Phys.–JETP* **36** 747
Kulik I O and Shekhter R I 1975 *Sov. Phys.–JETP* **41** 308
Averin D V and Likharev K K 1986 *J. Low. Temp. Phys.* **62** 345
[3] Erbe A, Blick R H, Tike A, Kriele A and Kotthaus J P 1998 *Appl. Phys. Lett.* **73** 3751
[4] Erbe A, Weiss C, Zwerger W and Blick R H 2001 *Phys. Rev. Lett.* **87** 096106–1
[5] Scheible D V, Erbe A and Blick R H 2002 *New J. Phys.* **4** 86
[6] Tuominen M T, Krotkov R V and Breuer M L 1999 *Phys. Rev. Lett.* **83** 3025
[7] Park H, Park J, Lim A K L, Anderson E H, Alivisatos A P and McEuen P L 2000 *Nature* **407** 57
[8] Gorelik L Y, Isacsson A, Voinova M V, Kasemo B, Shekhter R I and Jonson M 1998 *Phys. Rev. Lett.* **80** 4526
[9] Isacsson A, Gorelik L Y, Voinova M V, Kasemo B, Shekhter R I and Jonson M 1998 *Physica* B **255** 150
[10] Fedorets D, Gorelik L Y, Shekhter R I and Jonson M 2002 *Europhys. Lett.* **58** 99
[11] Nord T, Gorelik L Y, Shekhter R I and Jonson M 2002 *Phys. Rev.* B **65** 165312

[12] Weiss C and Zwerger W 1999 *Europhys. Lett.* **47** 97
[13] Nishiguchi N 2001 *Phys. Rev.* B **65** 035403-1
[14] Nishiguchi N 2001 *Japan. J. Appl. Phys.* **40** 1
[15] Nishiguchi N 2002 *Phys. Rev. Lett.* **89** 066802-1
[16] Keldysh L V 1965 *Sov. Phys.–JETP* **20** 1018
[17] Jauho A P, Wingreen N S and Meir Y 1994 *Phys. Rev.* B **50** 5528
[18] Boese D and Schoeller H 2001 *Europhys. Lett.* **54** 668
[19] McCarthy K D, Prokof'ev N and Tuominen M 2002 *Phys. Rev.* B submitted
(McCarthy K D, Prokof'ev N and Tuominen M 2002 *Preprint* cond-mat/0205419)
[20] Armour A D and MacKinnon A 2002 *Phys. Rev.* B **66** 035333
(Armour A D and MacKinnon A 2002 *Preprint* cond-mat/0204521)
(Armour A D and MacKinnon A 2002 *Preprint* cond-mat/0209216)
Armour A D and MacKinnon A 2002 *Physica* B **316/317** 403
[21] Persson S H M and Olofsson L 1996 *Appl. Phys. Lett.* **74** 2546
[22] Jaochim C, Gimzewski J K and Aviram A 2000 *Nature* **408** 541
[23] Gaudioso J, Lauhon L J and Ho W 2000 *Phys. Rev. Lett.* **85** 1918
[24] Majima Y, Nagano K and Okuda A 2002 *Japan. J. Appl. Phys.* **41** 5381
[25] Nagano K, Okuda A and Majima Y 2002 *Appl. Phys. Lett.* **81** 544
[26] Kubatkin S E, Danilov A V, Olin H and Claeson T 2000 *Phys. Rev. Lett.* **84** 5836
[27] Gorelik L Y, Isacsson A, Galperin Y M, Shekhter R I and Jonson M 2001 *Nature* **411** 454
[28] Isacsson A, Gorelik L Y, Shekhter R I, Galperin Y M and Jonson M 2002 *Phys. Rev. Lett.* **89** 277002
[29] Tuominen M T, Hergenrother J M, Tighe T S and Tinkham M 1992 *Phys. Rev. Lett.* **69** 1997
Tuominen M T, Hergenrother J M, Tighe T S and Tinkham M 1993 *Phys. Rev.* B **47** 11
Tuominen M T, Hergenrother J M, Tighe T S and Tinkham M 1993 *Phys. Rev.* B **47** 599
Hergenrother J M, Tuominen M T and Tinkham M 1994 *Phys. Rev. Lett.* **72** 1742
[30] Lafarge P, Joyez P, Esteve D, Urbina C and Devoret M H 1993 *Phys. Rev. Lett.* **70** 994
Eiles T M, Martinis J M and Devoret M H 1993 *Phys. Rev. Lett.* **70** 1862
Joyez P, Lafarge P, Filipe A, Esteve D and Devoret M H 1994 *Phys. Rev. Lett.* **72** 2458
[31] Matveev K, Gisselfält M, Glazman L I, Jonson M and Shekhter R I 1993 *Phys. Rev. Lett.* **70** 2940
Hekking F W J, Glazman L I, Matveev K and Shekhter R I 1993 *Phys. Rev. Lett.* **70** 4138
Matveev K A, Glazman L I and Shekhter R I 1994 *Mod. Phys. Lett.* B **8** 1007
Glazman L I, Hekking F W, Matveev K A and Shekhter R I 1994 *Physica* B **203** 316
[32] Nakamura Y, Pashkin Yu A and Tsai J S 1999 *Nature* **398** 786
[33] Vion D, Aassime A, Cottet A, Joyez P, Pothier H, Urbina C, Esteve D and Devoret M H 2002 *Science* **296** 886
[34] Makhlin Y, Schön G and Shnirman A 2001 *Rev. Mod. Phys.* **73** 357
[35] Shekhter R I, Gorelik L Y, Isacsson A, Galperin Y M and Jonson M 2001 *Proc. Nobel Jubilee Symp. on Coherence and Condensation in Condensed Matter (2001); Phys. Scr.* T **102** p 13
[36] Gorelik L Y, Isacsson A, Galperin Y M, Shekhter R I and Jonson M 2000 *Preprint* cond-mat/0012201
[37] Gorelik L Y, Shekhter R I, Vinokur V, Feldman D, Kozub V and Jonson M 2002 *Preprint* cond-mat/0211563
[38] Romito A, Plastina F and Faxio R 2002 *Preprint* cond-mat/0212414